



**HAL**  
open science

# **Exploring the deviations from scale-invariance of spatial distributions of buildings using a Geographically Weighted Fractal Analysis. An application to twenty French middle-size metropolitan areas**

François Sémécurbe, Cécile Tannier, Stephane G. Roux

## **► To cite this version:**

François Sémécurbe, Cécile Tannier, Stephane G. Roux. Exploring the deviations from scale-invariance of spatial distributions of buildings using a Geographically Weighted Fractal Analysis. An application to twenty French middle-size metropolitan areas. 2018. <hal-01708747>

**HAL Id: hal-01708747**

**<https://hal.science/hal-01708747v1>**

Preprint submitted on 14 Feb 2018

HAL is a multi-disciplinary open access archive for the deposit and dissemination of scientific research documents, whether they are published or not. The documents may come from teaching and research institutions in France or abroad, or from public or private research centers.

L'archive ouverte pluridisciplinaire HAL, est destinée au dépôt et à la diffusion de documents scientifiques de niveau recherche, publiés ou non, émanant des établissements d'enseignement et de recherche français ou étrangers, des laboratoires publics ou privés.



HAL Authorization

# Exploring the deviations from scale-invariance of spatial distributions of buildings using a Geographically Weighted Fractal Analysis. An application to twenty French middle-size metropolitan areas

**François Sémécurbe**

ThéMA, CNRS-Univ. Bourgogne Franche-Comté, Besançon, France.

**Cécile Tannier** (*corresponding author*)

Chrono-Environnement, CNRS-Univ. Bourgogne Franche-Comté, Besançon, France.

**Stéphane G. Roux**

Laboratoire de Physique, CNRS-Ecole Nationale Supérieure de Lyon, France.

## **Abstract.**

In the early twentieth century a handful of French geographers and historians famously suggested that mainland France comprised two agrarian systems: enclosed field systems with scattered settlements in the central and western France, and openfield systems with grouped settlements in eastern France. This division between grouped and scattered settlements can still be found on the outskirts of urban areas. The objective of this paper is to determine whether the shape of urban areas varies with the type of built patterns in their periphery. To this end, we identify and characterise the local and global deviations from scale-invariance of built patterns in metropolitan France. We propose a new method –Geographically Weighted Fractal Analysis – that can characterize built patterns at a fine spatial resolution without making any a priori distinction between urban patterns and suburban or rural patterns. By applying GWF to the spatial distribution of buildings throughout mainland France we identify six geographically consistent types of built patterns that are distinctive in the way buildings are either concentrated or dispersed across scales. The relationship between the local built textures and the global shape of twenty metropolitan areas is then analysed statistically. It is found that the proportion of dispersed (or concentrated) outer suburban built patterns in metropolitan areas is closely related to the distance threshold that marks the morphological limit of their urban areas.

**Keywords:** built textures, fractal analysis, suburban fringes, scale invariance, mainland France.

## **1. Introduction**

If we are to identify the advantages and disadvantages of different city shapes for various planning goals (e.g. preserving ecological connectivity, improving access to urban and rural amenities, ensuring good ventilation of the city centre, etc.) then – among other things – the associated urban built patterns need to be more accurately described and characterized. This need has engendered a wealth of publications describing and characterizing city shapes, including numerous methods of identifying different types of urban patterns along with many spatial indexes for measuring urban sprawl. In this paper, we seek to contribute to this field of research by exploring the multiscale morphological properties of urban built patterns in more depth.

In the early twentieth century, a number of renowned geographers and historians analysed the geography of rural France (Demangeon, 1927; Bloch, 1931; Dion, 1934). Their research led to a classical division of mainland France into two agrarian systems: enclosed field systems associated with scattered settlements in the centre and the West of France, and openfield systems associated with grouped settlements in the East of France. This distinction between grouped and scattered settlements can still be found on the periphery of urban areas. Obviously, the spatial expansion of cities does not take place within a blank, isotropic space, especially when cities belong to centuries-old settlement systems. As a consequence, built patterns in suburban fringes are somewhat hybrid: they blend inherited features (traditional rural buildings, land parcels, natural constraints) with new urban developments (most often, detached housing estates). This makes them difficult to describe and characterize. A number of publications have shown the value of fractal dimensions for characterizing irregular shapes of this kind. Fractal dimensions describe the way buildings are spatially distributed at several nested spatial resolutions. The closer the fractal dimension is to 2, the more uniform is the spatial distribution of buildings. In contrast, a fractal dimension close to 0 describes a highly concentrated spatial distribution of buildings at just a few locations across all scales. More often than not, buildings exhibit concentrated spatial configurations at some spatial resolutions and more dispersed patterns at other resolutions (fractal dimension in-between 1 and 2). Fractal analysis can be used to compare the built patterns of entire urban regions (Shen, 2002; Feng & Chen, 2010; Frankhauser, 2015) or smaller spatial units (neighbourhoods, communities) (Thomas, Frankhauser & Biernacki, 2008; Thomas et al., 2010).

As outer suburban areas are the space into which cities expand, it is to be expected that pre-existing suburban settlements will influence the shape of the urban development they come to accommodate. The objective of this paper is to determine whether the shape of French urban areas is determined by the shape of extant built-up areas on their outskirts. Analysis of the relationship between built-up shapes surrounding urban areas and the shape of the urban areas themselves first involves characterizing the built patterns at a fine spatial resolution, without making any a priori distinction between urban patterns and suburban or rural patterns. For this, we propose a new method, Geographically Weighted Fractal Analysis (GWFA). As with Geographically Weighted Regression (Brunsdon, Fotheringham & Charlton, 1996; Fotheringham, Brunsdon & Charlton, 2003), GWFA uses a mathematical kernel that describes the way the neighbourhood of a point is taken into account to estimate the fractal dimension of that point. By applying GWFA to French built patterns and classifying the results we have been able to map the built textures of France at a spatial resolution of 2000 m. Next, we compare the built textures thus mapped with the global shape of twenty metropolitan areas. For this, we choose to apply the method proposed by Tannier et al. (2011) to detect discontinuities in space across scales. This method can determine a distance threshold specific to each area under study. The statistical comparison of this distance threshold with the local built textures resulting from GWFA indicates whether or not the global shape of French metropolitan areas varies with the built shapes in their periphery.

## 2. Data and method

Source data are from the vector data to the nearest 1 m provided by the French cartographical service, BD Topo ® IGN 2011. This represents about 24 million buildings. For the analysis, each building is represented by its centroid in order to reduce both the size of the data base and the computation time.

In order to analyze these very detailed data, a four-steps methodology has been defined. It takes into account three guiding principles: 1) introducing no a priori distinction between urban patterns and suburban or rural patterns; 2) focusing the analyses on the deviations from scale invariance; 3) examining and confronting both global and local deviations from scale invariance.

**Step 1.** *Using GWFA (Geographically Weighted Fractal Analysis) to determining if the spatial distribution of buildings in metropolitan France is locally scale-invariant or not.*

Analysis is based on a 2000 m-spaced grid of 145,178 estimation points  $i$  that covers the whole country. On this basis, GWFA (see section 3) is used to estimate the fractal dimension at each point  $i$  of the study area. Fractal dimensions describe the way buildings are spatially distributed at several nested spatial resolutions. The underlying assumption is that the spatial distribution of buildings is scale invariant, which means that the variation in the built density from one given spatial resolution to another is constant across scales. The scale invariance is proven when the goodness-of-fit of the estimation of the fractal dimension is satisfactory. This goodness-of-fit is usually very high when estimating fractal dimensions. Therefore,  $R^2$  values between 0.95 and 0.995 do not guarantee scale invariance for the whole scale range, and  $R^2$  values less than 0.95 are sure signs of a disruption in scale invariance.

**Step 2.** *Identifying different types of built patterns according to the way the spatial distribution of buildings deviates locally from a scale-invariant distribution.*

Here the spatial distribution of buildings at each point  $i$  is not supposed to be scale invariant and each point  $i$  is characterized by a series of scaling indexes  $Sc$  calculated for successive scale intervals. These  $Sc$  indexes correspond to the  $\alpha(\epsilon)$  indexes used by Thomas et al. (2010) to characterize the scaling behaviour of built patterns of European urban wards.

In order to analyse the profile of  $Sc$  indexes for each point  $i$ , we applied a Principal Component Analysis. Then we classified the 145,178 points  $i$  according to their two coordinates on the PCA axes using the k-means method.

**Step 3.** *For a selection of twenty French metropolitan areas, characterizing the global deviation of the spatial distribution of buildings from a scale-invariant distribution. For this, calculation of a distance threshold that indicates a crucial discontinuity in space across scales.*

For this, we use the free software application named MorphoLim (<https://sourcesup.renater.fr/morpholim/>) to perform the method proposed by Tannier et al.

(2011). By this method a dilation of each individual building is first applied, then a distance threshold is detected on the dilation curve. This distance threshold corresponds to the dilation step at which the curve deviates the most from a straight-line. At this point on the dilation curve, distances separating buildings no longer exhibit the same fractal behaviour. Thus this point indicates the maximum morphological difference between the inlying built patterns (i.e. the morphological agglomeration) and the outlying built patterns (i.e. the surrounding suburban areas). The distance threshold is specific to each area under study: the less an urban area differs morphologically from its surrounding built landscape (in terms of variations in distances separating buildings), the greater the distance threshold; the fewer the buildings in a study area that are connected across scales, the greater the distance threshold.

**Step 4.** *For the twenty selected French metropolitan areas, making a statistical comparison of the distance threshold that characterizes globally the spatial distribution of buildings across scales with the dominant types of local built textures identified at step 2.*

### 3. Geographically Weighted Fractal Analysis: detailed description

The fractal dimension  $D$  of an object is defined through a scaling function  $F_\epsilon$  that describes an aspect of the spatial distribution of the points  $e$  of the object.

$$F_\epsilon \sim \epsilon^{-D} \text{ where } \epsilon \text{ is the size of the counting window} \quad (1)$$

For theoretical mathematical objects,  $D$  corresponds to the asymptotic behaviour of  $F_\epsilon$  when  $\epsilon$  tends to 0. For real world objects,  $D$  is estimated for the range of scales  $\epsilon$  for which the points of the curve of  $\log(F_\epsilon)$  with respect to  $-\log(\epsilon)$  form a straight line.  $D$  is the slope of this straight line.

Each scaling function  $F_\epsilon$  enables the calculation of a given fractal dimension. The chosen scaling function for Geographically Weighted Fractal Analysis (GWFA) is  $M_r^q$ , where  $r$  corresponds to  $\epsilon$  and  $M$  corresponds to  $F$ .

$$M_r^q \sim r^{Dq} \quad (2)$$

For a given point  $e$ ,  $M_r(e)$  is the number of points within a distance  $r$  around  $e$ .  $M_r^q$  is obtained by aggregating the  $M_r(e)$  of all points  $e$ . When a simple average is used for the aggregation, the fractal dimension obtained is the correlation dimension (Grassberger & Procaccia, 1983). In contrast, when a mathematical norm is used for the aggregation (eq. 3), the fractal dimension obtained is a multifractal generalized dimension  $D_q$ . The corresponding estimation method is the sandbox method (Vicsek, 1990).

$$M_r^q = \left[ \frac{1}{n} \sum_e M_r(e)^{q-1} \right]^{\frac{1}{q-1}} \sim r^{D_q} \quad (3)$$

The parameter  $q$  controls the nature of the aggregation: more importance is given either to high values of  $M_r(e)$ , when  $q$  is high, or to low values of  $M_r(e)$ , when  $q$  is low. In GWFA,  $q$  is set to 0 meaning that high or low values of  $M_r(e)$  all have the same importance. The corresponding generalized dimension  $M_r^0$  is closely related to, but more reliable than, the well-known box-counting dimension (Tél, Fulop & Vicsek, 1989; Vicsek, 1990). On this basis, GWFA is defined as:

$$M_r(i) = \left[ \sum_e (W_{i,e} M_r(e))^{-1} \right]^{-1} \sim r^{D_0} \quad (4)$$

In eq. 4, we see that weights  $W_{i,e}$  are attributed to the  $M_r(e)$  values. Each weight corresponds to the distance of the point  $e$  under consideration to a focus point  $i$ , also called the estimation point (**Figure 1**). Thus GWFA introduces distance-based weights assigned to each pair of points  $(i,e)$  in the calculation of the scaling function  $M_r(i)$ . By doing this, the measures provided by GWFA are local and not global.

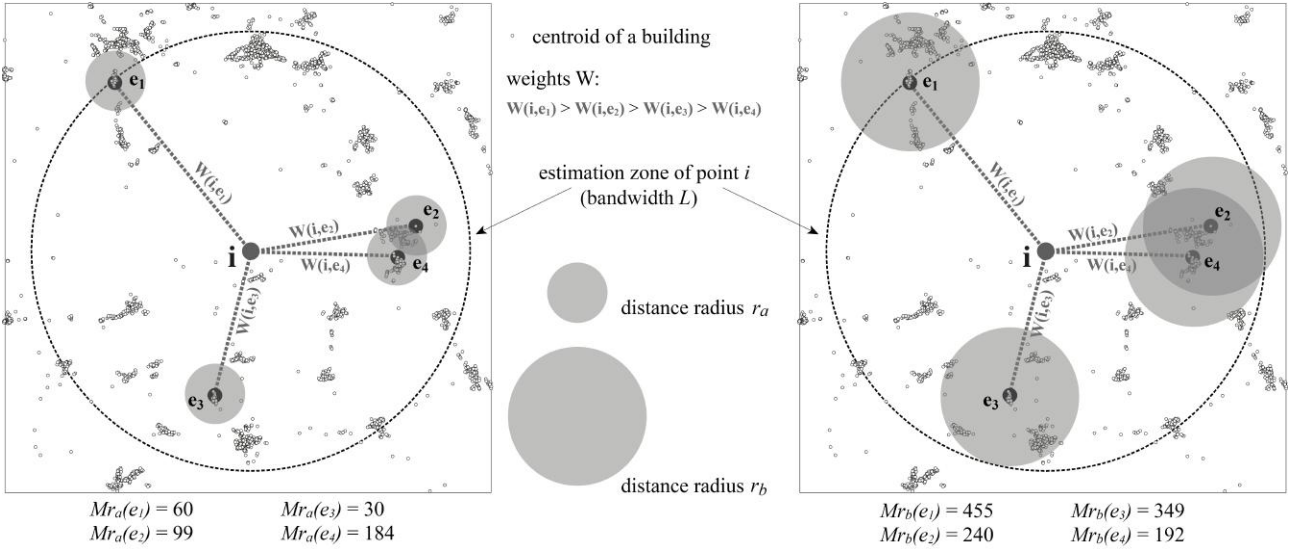


**Figure 1.** Counting variables

Weights  $W_{i,e}$  are calculated by applying a mathematical positive kernel  $K$ :

$$W_{i,e} = K(d_{ie} / L)$$

where  $d_{ie}$  is the distance between the estimation point  $i$  and the observation  $e$ ;  $L$  is the bandwidth of the analysis.

For GWFA, the quartic (bi-weight) kernel is used (**Figure 2**).

$$K(x) = (1 - x^2)^2, \text{ if } x < 1,$$

and 0, otherwise

The quartic kernel resembles the Gaussian kernel but has a compact support and enables faster computation. In any event, a positive, continuous and decreasing kernel that tends asymptotically to 0 ensures regular and continuous estimations in space, which enables results to be mapped satisfactorily (Brunsdon, Fotheringham & Charlton, 1996).

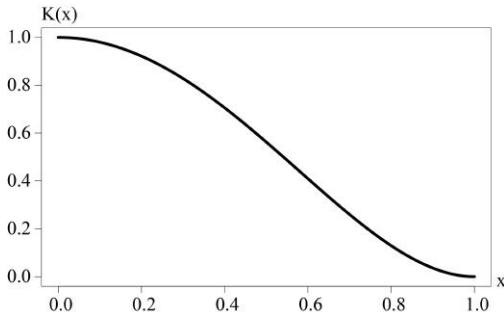


**Figure 2.** Quartic kernel

$M_r(e)$  values for points  $e$  close to  $i$  have a higher weight in the estimation of  $M_r(i)$  than  $M_r(e)$  values for points  $e$  that lie far from  $i$ . Moreover, when  $L$  is small, the analysis is very local. Contrarily, when  $L$  corresponds almost to the length the object under study, the analysis is global. Points counted for each  $M_r(e)$  may be located outside the bandwidth  $L$  but have to belong to the object under study. In this way, boundary effects related to points  $e$  located close to the boundary of the bandwidth  $L$  are avoided.

The fractal dimension  $D_0$  is obtained by estimating the slope of the curve of  $\log(M_r(i))$  with respect to  $\log(r)$  for a given set of radii  $r$  by OLS (ordinary least squares) regression. This fractal dimension is calculated in step 1 of the methodology exposed in section 2.  $Sc$  indexes calculated in step 2 are defined as the differences in the logarithms of two scaling functions calculated for two successive scale ranges, e.g.:

$$Sc_{100-50} = \log(M_{100}(i)) - \log(M_{50}(i)) \quad (5)$$

The underlying hypothesis is that intermediate points between the two target points, e.g.  $\log(M_{100}(i))$  and  $\log(M_{50}(i))$ , lie on a straight line. In other words, the scale invariance is assumed to exist within the scale range 50–100 m.

In order to analyse the built patterns of the whole of metropolitan France, GWFA is applied on a 2000 m-spaced grid of 145,178 estimation points  $i$ . A distance of 2000 m between any two estimation points  $i$  is small enough to analyse local variations in fractal behaviour. At the same time, a distance of 2000 m is large enough to obtain a reliable estimation of fractal dimension for scales ranging from 0 to 800 m (see below).

The bandwidth  $L$  around each estimation point  $i$  has to be larger than the distance between two neighbouring points  $i$  in order to enable the analysis of built textures in an almost continuous way. Accordingly,  $L$  is set at 8000 m. Thus it includes two neighbouring estimation points  $i$  around a given point  $i$  in each direction.

Five distances  $r$  are considered: 50, 100, 200, 400, and 800 m. As the target estimated curve is a straight line, five points are enough to perform a statistical estimation of the fractal dimension that is reliable. Thus introducing additional distances  $r$  between 50 and 800 m. is useless. Of course, standard errors of the estimates may be rather large but if they are, this shows that the spatial distribution of buildings is locally not scale-invariant. The 1:10 ratio between  $r = 800$  and  $L = 8000$  ensures that the statistical estimations of fractal dimensions are robust. In addition, 100 circles of radius  $r = 800$  m can entirely cover each estimation zone of radius  $L$  around  $i$ . Introducing additional distances  $r$  larger than 800 m. would not be relevant because this would create boundary effects. Introducing additional distances  $r$  lower than 50 m. would also not be relevant because each point  $e$  corresponds to the centroid of a building but not to its real spatial footprint.

On average, each zone of radius  $L$  around each estimation point  $i$  contains 8600 centroids of buildings. To reduce the computation time required for calculating  $M_r(e)$  values, only 3000 points  $e$  are selected randomly among all centroids of buildings around each estimation point  $i$ . If a zone contains fewer than 3000 points  $e$ , all those points are taken into account. This sample size (3000) is large enough to detect zones that are almost entirely covered by buildings, namely dense intra-urban zones. Moreover, with a radius  $r$  equal to 800 m. and with 3000 points  $e$ , each centroid of building is taken into account at least one time in the calculation.

In order to perform all calculations easily, an R package entitled GWFA has been created. Input data are two files, one containing the estimation points  $i$  with their XY coordinates and the other containing building centroids  $e$  with their XY coordinates.

## 4. Results

### 4.1 Estimated fractal dimensions with GWFA show local deviations from scale-invariance, especially in the West and South-West of France

By applying GWFA to the building centroids for the whole of metropolitan France, local fractal dimensions were computed on the basis of the five distance radii  $r$  (50, 100, 200, 400, and 800 m) (**Figure 3a**).

**Figure 3b** shows that most places in central and western France exhibit  $R^2$  values of less than 0.95. Thus, the spatial distribution of buildings there is not scale invariant. The goodness-of-fit of the estimation is higher than 0.95 only in eastern France and in the largest urban areas (**Figure 4**).

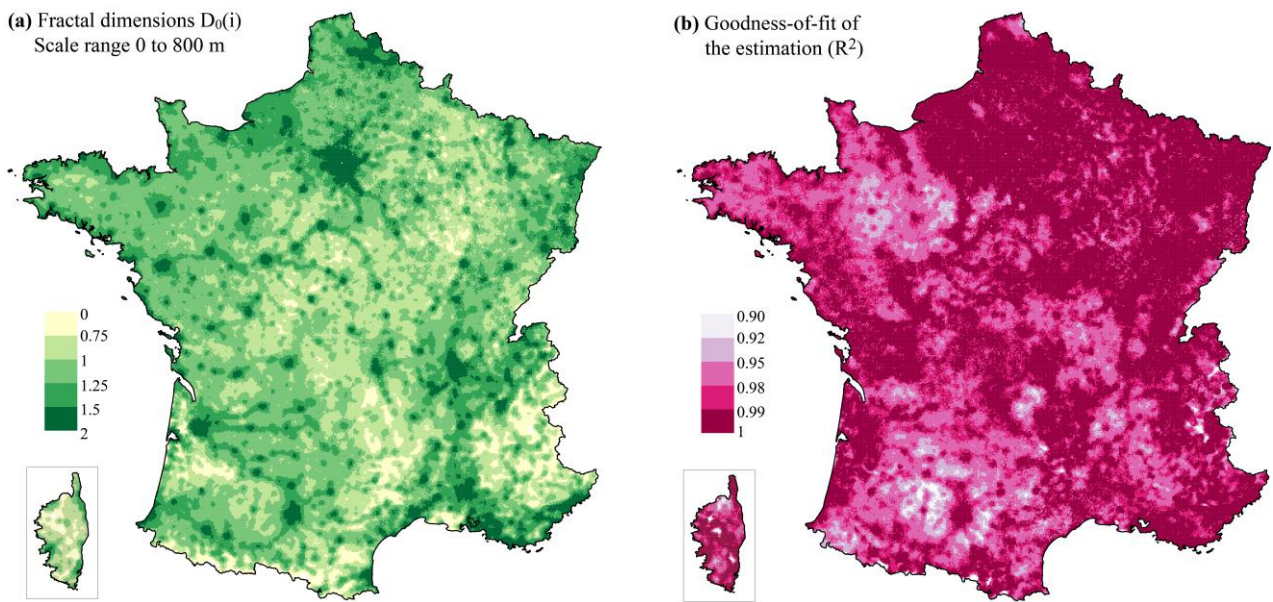


**Figure 3.** Fractal dimensions estimated for the scale range 0 to 800 m. 145,178 estimation points  $i$ . On the maps, each estimation point corresponds to a 2000 m-wide square spatial unit.

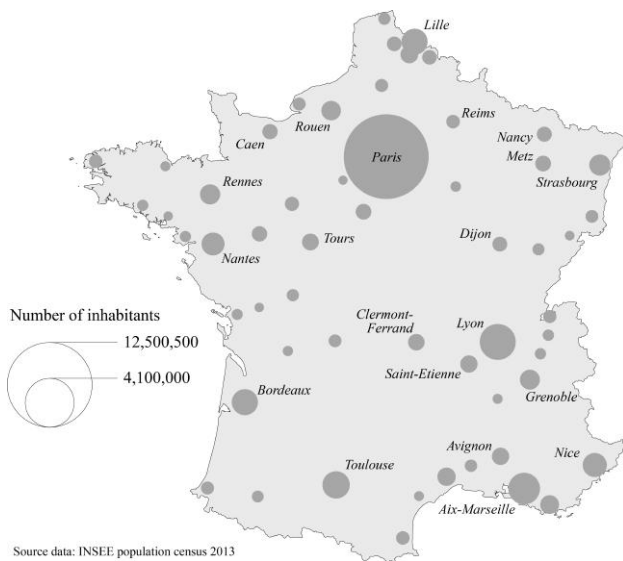


**Figure 4.** Most populated metropolitan areas of mainland France.

Considering this, we estimated two other fractal dimensions, one for distance radii  $r$  50, 100, and 200 m and another for distance radii  $r$  200, 400, and 800 m. As expected, these two fractal dimensions are clearly different for places located outside the main urban areas in the West and South-West of France: in those places, estimated fractal dimensions are low for  $r$  50, 100, and 200 m, but high for  $r$  200, 400, and 800 m (Figures 5a and 5b).

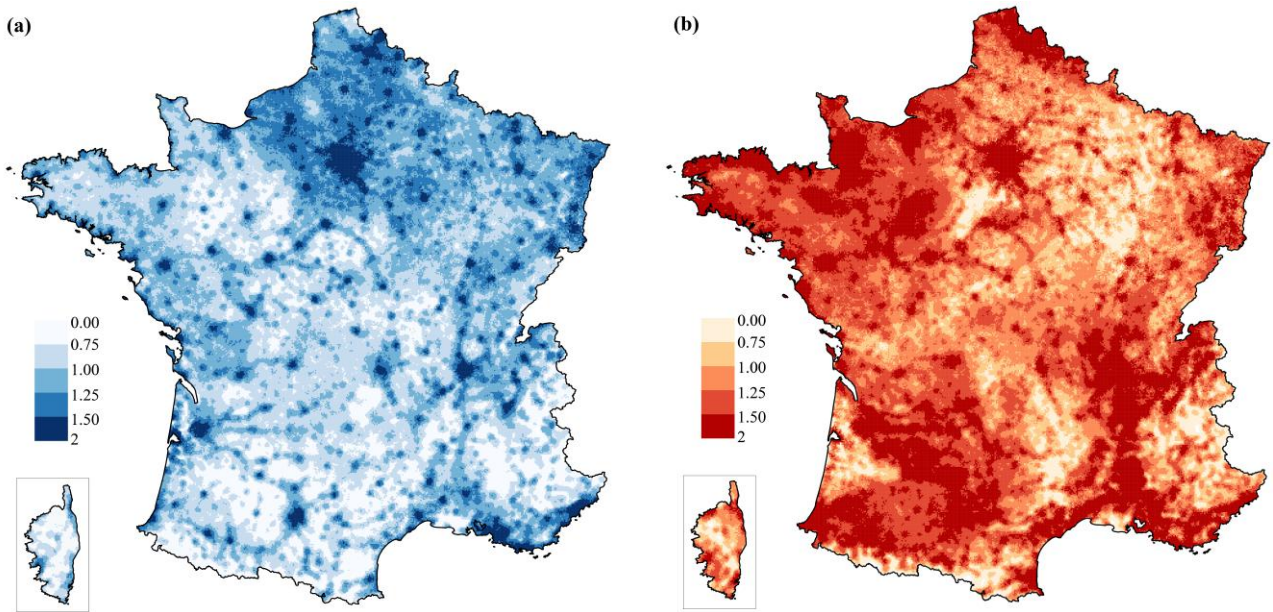


**Figure 5.** Fractal dimensions estimated for the distance radii (a) 50, 100, and 200 m, and (b) 200, 400, and 800 m.

These results suggest that estimating one fractal dimension for the entire scale range (**Figure 3**) or two fractal dimensions for two smaller scale ranges (**Figure 5**) does not enable us to characterize the spatial distribution of buildings in each zone around  $i$  precisely enough.

#### 4.2 Typology of local built textures built on scaling indexes $Sc$

With five distance radii  $r$ , it is possible to calculate four scaling indexes  $Sc$ . In order to analyse them simultaneously, we applied a Principal Component Analysis (**Figure 6**). Two additional variables (not taken into account in the PCA) have been represented on the circle of correlation: the fractal dimension as calculated for **Figure 3a** and the logarithm of the built density. The two first components of the PCA concentrate 90% of the total inertia.

The first component contrasts areas characterized by a low fractal dimension and a low built density (*i.e.* rural areas) with areas characterized by a high fractal dimension and a high built density (*i.e.* urban areas) (**Figure 7a**). On the circle of correlations, we observe that this first principal component is strongly correlated with the four  $Sc$  indexes, all oriented in the same direction with respect to the first axis. Moreover, the two additional variables (fractal dimension and built density) are strongly correlated to this axis.

The second component of the PCA reflects the fact that a built pattern may or may not exhibit a scale-invariant distribution across all scale ranges, from 0 to 800 m. It orders the scaling indexes in accordance with their distance radii: on the circle of correlations,  $Sc_{100-50}$  and  $Sc_{200-100}$  lie very close to each other and far from  $Sc_{800-400}$ ;  $Sc_{400-200}$  lies in an intermediate position. In **Figure 7b**, we see that the coordinate of urban areas is close to 0 for this second component. Indeed, their spatial

organization is scale-invariant across the whole scale range (from 0 to 800 m) and, consequently, the four indexes  $Sc$  have almost the same values. Contrarily, the values of the scaling indexes vary with the distance radii for peripheral areas in the West of France, which appear in red in **Figure 7b**: obviously, their fractal dimension is low in **Figure 5a** and high in **Figure 5b**. This stark contrast is explained by the dispersion of clusters of buildings, namely small villages and hamlets: for large distance radii (0–400 and 0–800 m), all points  $e$  have numerous neighbours and the index  $Sc_{800-400}$  is high; conversely, for small distance radii, many points  $e$  have almost no neighbours and the indexes  $Sc_{100-50}$  and  $Sc_{200-100}$  are low. Built patterns in blue in **Figure 7b** exhibit a more complex scaling behaviour because they are locally more concentrated. For distance radii 0–50 m and 0–100 m, each point  $e$  has numerous neighbours located within the same built cluster and the index  $Sc_{100-50}$  is high. Then, for distance radii 0–200 m and 0–400 m, there are relatively fewer neighbours of each point  $e$ ; they belong either to the built cluster of point  $e$  or to other built clusters (neighbouring villages) but the probability of finding other villages in the vicinity of the village of point  $e$  is low for such distances. The value of indexes  $Sc_{200-100}$  and  $Sc_{400-200}$  are accordingly lower. Finally, for large distance radii (0–400 and 0–800), the probability of finding neighbouring villages is much higher and the value of index  $Sc_{800-400}$  is also higher.

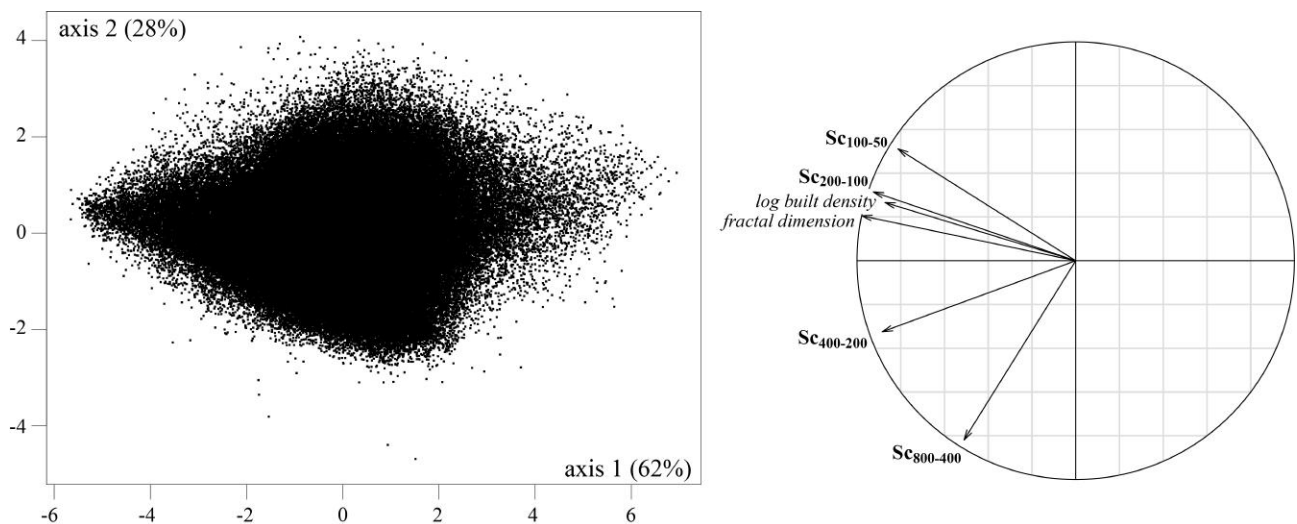


**Figure 6.** Results of the Principal Component Analysis. Four variables:  $Sc_{100-50}$ ,  $Sc_{200-100}$ ,  $Sc_{400-200}$ , and  $Sc_{800-400}$ ; 145,178 individuals: 2000 m-wide square spatial units.

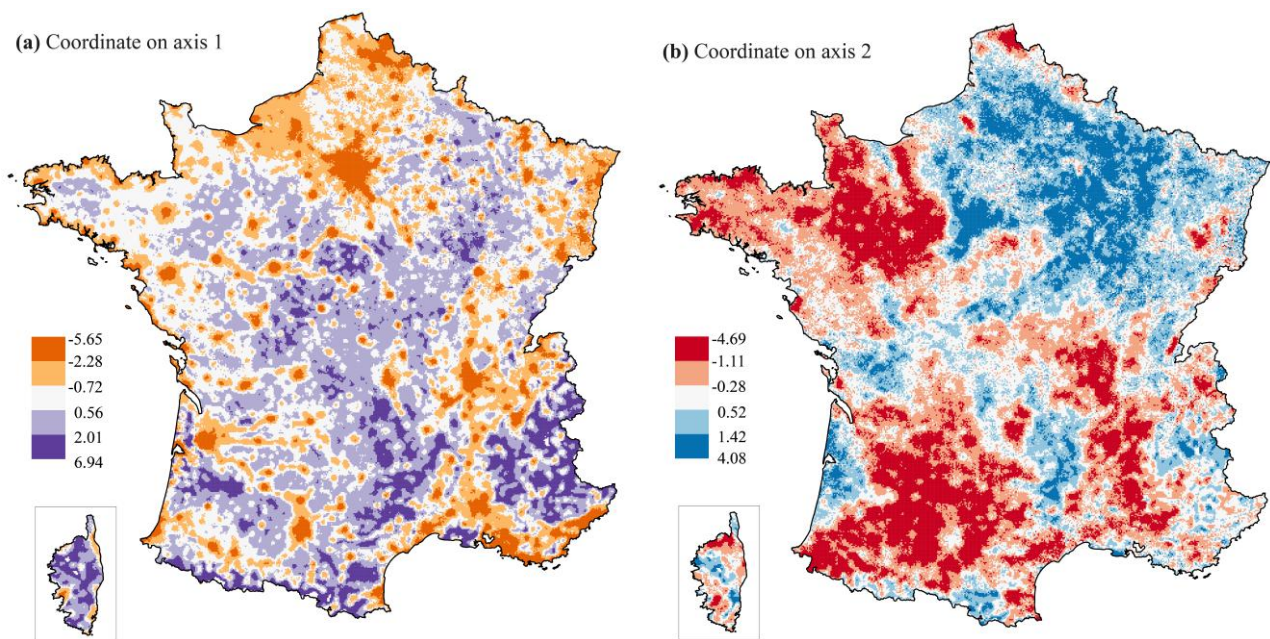


**Figure 7.** Coordinates of each 2000 m-wide zone  $i$  on the two first axes of the PCA.

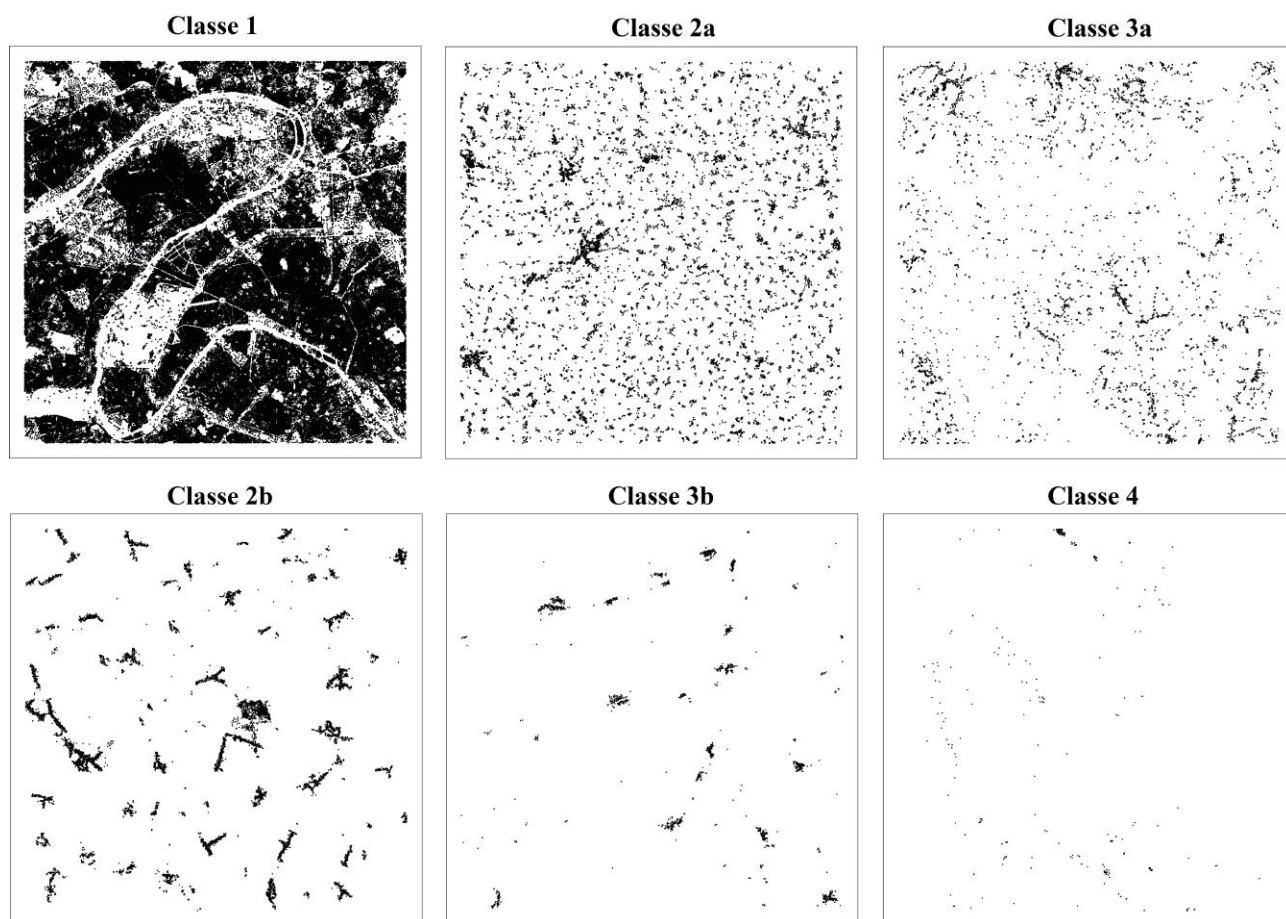


**Figure 8.** Built pattern typical of each class.

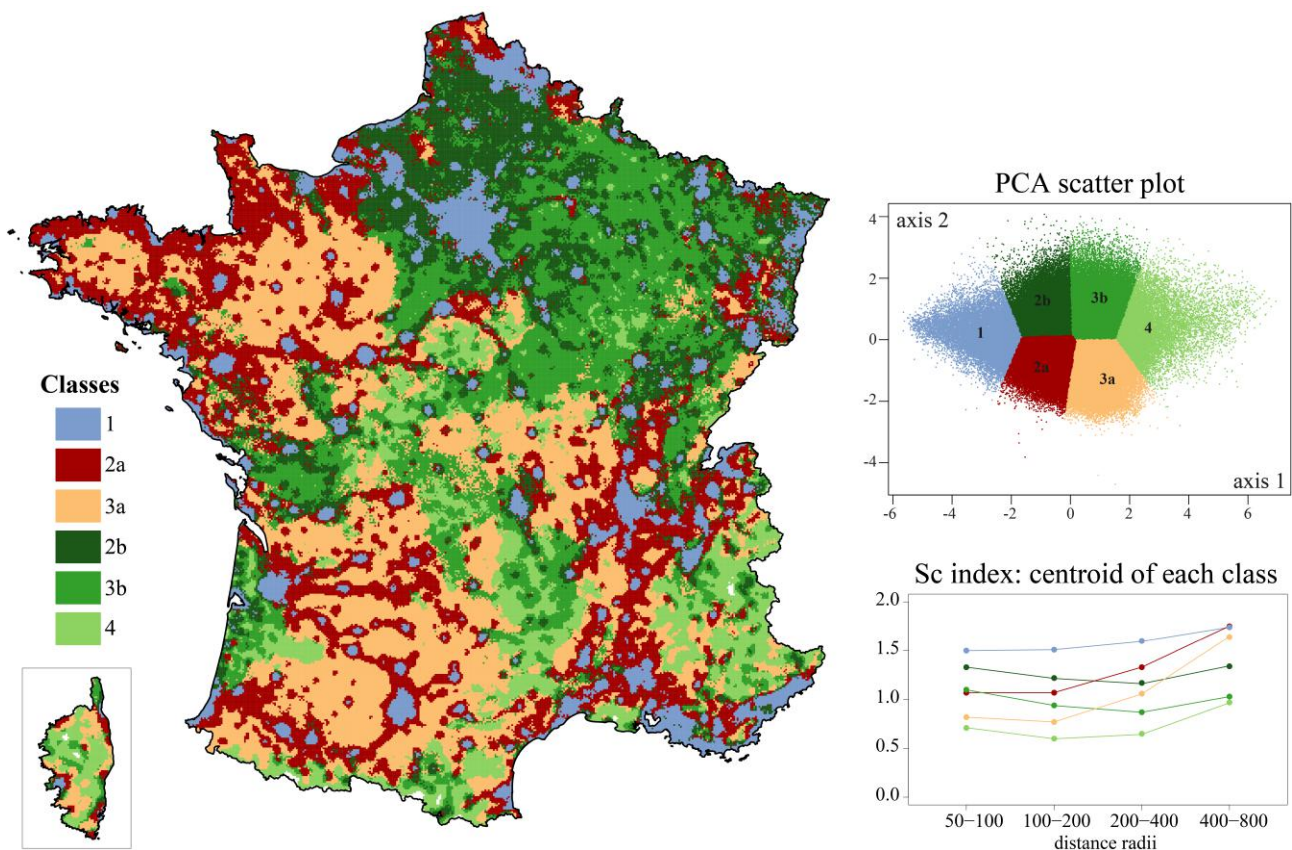


**Figure 9.** Typology of built patterns according to their multiscale behaviour.

Finally, we classified the 145,178 spatial units according to their two coordinates on the PCA axes using the k-means method. Six classes of built textures have been identified (**Figure 8**). Classes 1 and 4, which occupy contrasting positions on the first axis of the PCA, are separated in the classification from classes 2a, 2b, 3a, and 3b. Classes 2 (a and b) and classes 3 (a and b) are also separated since they occupy contrasting positions on the first axis of the PCA. Simultaneously, classes a (2 and 3) and classes b (2 and 3) are separated since they occupy contrasting positions on the second axis of the PCA. As shown on Figure 9, classes 2a and 3a correspond to locally dispersed built patterns. They are more scattered and diffuse in class 3a than in class 2a. Classes 2b and 3b correspond to locally concentrated built patterns; villages in class 2b are larger and more numerous than in class 3b.

The resulting typology map is well structured although no contiguity criterion has been introduced into the classification (**Figure 9**). Clusters of spatial units belonging to a same class are very consistent: class 1 spatial units are urban areas; class 4 spatial units are sparsely populated areas; class 2a, 2b, 3a, and 3b spatial units are located in the periphery of urban areas.

### 4.3 For twenty middle-size metropolitan areas, identification of the distance threshold that characterizes globally how the spatial distribution of buildings deviates from scale invariance

For the purpose of the analysis, we used the delineation of French *aires urbaines* (metropolitan areas) (Figure 10), which encompass a densely built urban area and its commuter belt. We chose to consider neither large metropolitan areas because they encompass several *aires urbaines* that are sometimes spatially separated, nor small metropolitan areas as they do not contain enough 2000 m-wide spatial units.

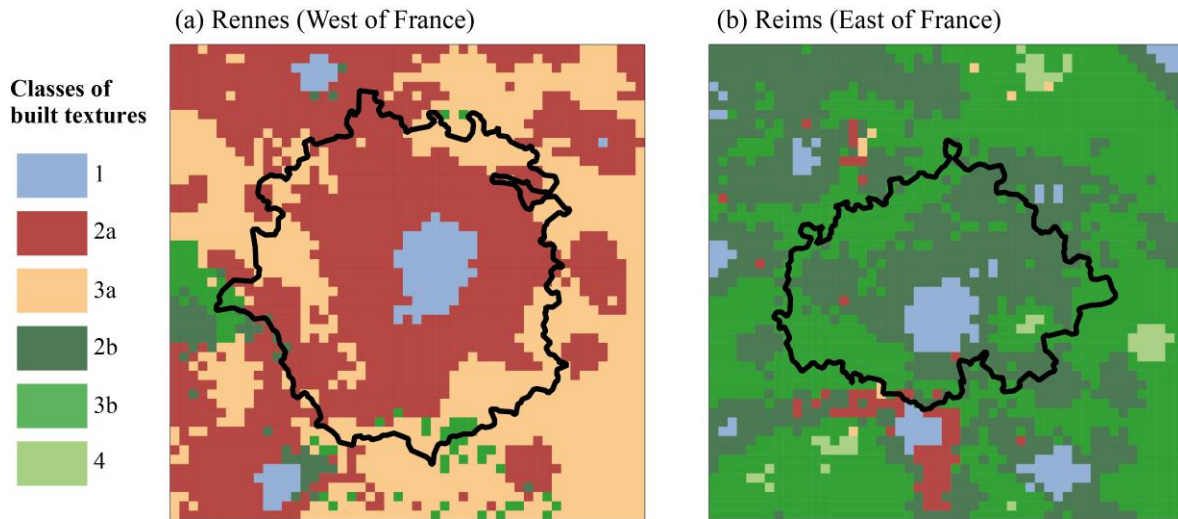


**Figure 10.** Two metropolitan areas and their built textures. Black line: limit of the metropolitan area (*aire urbaine*).

Within the perimeter of each metropolitan area, a distance threshold that indicates a crucial discontinuity in space across scales was identified using the MorphoLim software application. This distance threshold indicates the maximum morphological difference between the built patterns that belong to the urban area (i.e. the morphological agglomeration) and the outlying built patterns (i.e. the surrounding suburban areas). Table 1 shows that this distance threshold varies markedly among cities, from 78 m. for Avignon (South of France) to 529 m. for Troyes (East of France).

**Table 1.** Morphological characteristics of 20 French metropolitan areas.

Name of the metropolitan area	Distance threshold (m)	% of spatial units exhibiting locally dispersed built patterns (classes 2a and 3a)	% of spatial units exhibiting locally concentrated built patterns (classes 2b and 3b)
Avignon	78	52	4
Angers	127	88	2
Bayonne	143	68	0
Le Mans	143	91	0
Rennes	143	90	3
Vannes	165	71	13
Nantes	171	73	12
Caen	181	49	27

Name of the metropolitan area	Distance threshold (m)	% of spatial units exhibiting locally dispersed built patterns (classes 2a and 3a)	% of spatial units exhibiting locally concentrated built patterns (classes 2b and 3b)
Poitiers	207	24	58
Clermont-Ferrand	242	24	56
Niort	245	22	66
Bourges	256	10	78
Nancy	290	8	77
Orléans	318	35	45
Metz	389	3	75
Amiens	395	4	89
Dijon	415	4	83
Saint-Quentin	420	0	86
Reims	434	1	90
Troyes	529	2	90

#### 4.4 Comparison of local built patterns with the global shape of metropolitan areas

Tables 1 and 2 show that the proportion of dispersed (or alternatively concentrated) suburban built patterns in metropolitan areas is closely related to their global shape, i.e. their distance threshold. The more the suburban built patterns are dispersed into numerous, regularly spaced, small villages and hamlets, the smaller the distance threshold; the more the suburban built patterns are locally concentrated within large villages, the greater the distance threshold. This clearly confirms the hypothesis that the shape of French urban areas strongly depends on the built-up shapes in their periphery. Conversely, neither the proportion of spatial units in classes 1 (urban areas) and 4 (sparsely populated areas) nor the area of the metropolitan areas are correlated with the distance threshold.

**Table 2.** Statistical correlation between the distance threshold characterizing each urban area and other morphological characteristics. 20 metropolitan areas. p-values \*\*\*  $p < 0.001$  \*\*  $p < 0.01$  \*  $p < 0.05$ .

Variable	Pearson correlation coefficient
% of spatial units in classes 2a and 3a (dispersed built pattern)	-0.84***
% of spatial units in class 2a	-0.84***
% of spatial units in class 3a	-0.69***
% of spatial units in classes 2b and 3b (concentrated built pattern)	0.89***
% of spatial units in class 2b	0.81***
% of spatial units in class 3b	0.62**
% of spatial units in class 1	-0.46*
% of spatial units in class 4	0.10
Area of the metropolitan area	-0.03

## 5. Discussion

The classification of scaling indexes obtained with GWFA has enabled the identification of six types of built patterns whose multiscale spatial organization is well differentiated. Sémécurbe, Tannier & Roux (2016) have previously identified similar types of settlement patterns by applying a multifractal analysis on fine-grained population data. That previous study was coarser-grained as mainland France was divided into 992 square spatial units 25 km wide (the present study considered 145,178 estimation points  $i$  2 km apart). The method was also different: the typology (a Hierarchical Ascending Classification) was based on the multifractal spectra of each spatial unit. Interestingly, despite the differences in methods and spatial resolutions, those two studies detected the same phenomena. In particular, the map displaying the value of each point  $i$  on the first axis of the PCA in the present study, which contrasts areas characterized by a low fractal dimension and a low built density (*i.e.* rural areas) and areas characterized by a high fractal dimension and a high built density (*i.e.* urban areas) (**Figure 7a**), resembles the map of generalized fractal dimension of order  $q = 2$  that highlights the strongest spatial singularities (Figure 3d in (Sémécurbe, Tannier & Roux 2016)). It should be recalled here that GWFA calculates a generalized fractal dimension of order  $q = 0$ . Conversely, the map displaying the value of each estimation point  $i$  on the second axis of the PCA in the present study (**Figure 7b** that highlights the deviation with respect to scale invariance) resembles the map of generalized fractal dimension  $D$  of order  $q = 0$  for which only the presence or absence of population in each cell is taken into account (Figure 3b in (Sémécurbe, Tannier & Roux, 2016)). Thus, the two studies look at the same phenomena, namely the concentration and dispersion of human settlements at several scales, from two different points of view, namely the departure from scale invariance in the present paper and the more or less multifractal aspect of the spatial distribution in (Sémécurbe, Tannier & Roux, 2016).

One point of interest in the present study is that the relatively small size of elementary spatial units (2000 m-wide) has allowed us to compare and contrast the local built textures with the global shape of cities (*i.e.* their distance threshold). Because of the use of both a k-means classification and the MorphoLim method, the results obtained may be specific to mainland France: on the one hand, the result of the statistical classification of built textures depends on the diversity of built textures within the study area (in mainland France, the built textures are highly contrasted); on the other hand, the distance threshold characterizing each urban area depends on the definition of metropolitan areas, which may vary among countries. Thus it would be interesting to apply the methodology proposed in this paper to analyse built patterns in other countries, with a view to making international comparisons.

## 6. Conclusion

In this paper, we have proposed a new method for spatial analysis, namely Geographically Weighted Fractal Analysis. We have used it to explore the local deviations from scale-invariance of spatial distributions of buildings in the whole of mainland France. Its application, without making any a priori distinction between urban patterns and suburban or rural patterns and without imposing

any contiguity criterion, has enabled the identification of six geographically consistent built patterns that differ in the way buildings are concentrated and dispersed across scales. Then, for twenty middle-size metropolitan areas, we have compared the local built textures with the distance threshold that characterises globally the spatial distribution of buildings. This comparison has shown that the global shape of cities is closely related to their surrounding built patterns: the urban sprawl process has affected places differently according to their pre-existing rural built patterns (typically, numerous small dispersed hamlets or fewer large villages), which correspond to centuries-old agrarian systems (typically, enclosed field systems and openfield systems).

The fact that outer suburban patterns are inherited (in part at least) from past settlement patterns is well recognized: like many complex systems, settlement systems are generally characterized by strong path dependency (Andersson, 2008). Nevertheless, in some cases, the urban sprawl process has not preserved features of old agrarian systems but has made a more or less clean sweep of pre-existing rural built patterns. For instance in the Champagne-Ardenne region of France, when land was controlled by cereal farmers and winegrowers, residential developments occurred mainly as extensions to the larger villages. Conversely, housing estates with stereotyped architecture were constructed where successive land reparation made sites available or where farmers were behind the projects so as to cash in on their landholdings or prepare for their retirement (Mancebo & Salles, 2014). Such spatial variation in the intensity of path dependency could be explored quantitatively by applying the method and tools proposed in this paper.

## References

- Andersson, C. (2008). Ontogeny and ontology in complex systems modeling. In S. Albeverio, D. Andrey, P. Giordano & A. Vancheri, eds, *The Dynamics of Complex Urban Systems: An Interdisciplinary Approach*, Physica-Verlag, 43–58.
- Brunsdon, C., Fotheringham, A. S. & Charlton, M. (1996). Geographically Weighted Regression: A Method for Exploring Spatial Nonstationarity, *Geographical Analysis*, 28(4), 281–298.
- Bloch, M. (1931). *Les caractères originaux de l'histoire rurale française*. Oslo: Instituttet for sammenlignende kulturforskning.
- Brunsdon, C., Fotheringham, A. S. & Charlton, M. E. (1996). Geographically weighted regression: a method for exploring spatial nonstationarity. *Geographical Analysis*, 28(4), 281–298.
- Demangeon, A. (1927). La géographie de l'habitat rural. *Annales de Géographie*, 36, 1–23.
- Dion, R. (1934). *Essai sur la formation du paysage rural français*. Tours, France: Arrault.
- Feng, J. & Chen, Y. (2010). Spatiotemporal evolution of urban form and land-use structure in Hangzhou, China: Evidence from fractals. *Environment and Planning B: Planning and Design*, 37(5), 838–856.
- Fotheringham, A. S., Brunsdon, C. & Charlton, M. (2003). *Geographically Weighted Regression: The Analysis of Spatially Varying Relationships*, John Wiley & Sons.
- Frankhauser, P. (2015). From fractal urban pattern analysis to fractal urban planning concepts. In: M. Helbich, J. Jokar Arsanjani & M. Leitner. *Computational Approaches for Urban Environments, Geotechnologies and the Environment*, Springer, pp.13–48.

- Mancebo, F. & Salles, S. (2014). De l'autre côté du miroir. Un périurbain pensé par le rural, pour une périurbanisation modelée par les usages. *Premier plan Le journal d'informations du PUCA (plan urbanisme construction architecture)*, 30, 4–6.
- Grassberger, P. & Procaccia, I. (1983). Measuring the strangeness of strange attractors. *Physica D*, 9, 189–208.
- Sémécurbe, F., Tannier, C. & Roux, S. G. (2016). Spatial distribution of human population in France: exploring the Modifiable Areal Unit Problem using multifractal analysis. *Geographical Analysis*, 48(3), 292–313.
- Shen, G. (2002). Fractal dimension and fractal growth of urbanized areas. *International Journal of Geographical Information Science*, 16(5), 437–519.
- Tannier, C., Thomas, I., Vuidel, G. & Frankhauser P. (2011). A fractal approach to identifying urban boundaries. *Geographical Analysis*, 43(2), 211–227.
- Tél, T., Fülöp, Á. & Vicsek, T. (1989). Determination of fractal dimensions for geometrical multifractals. *Physica A: Statistical Mechanics and its Applications*, 159(2), 155–166.
- Thomas, I., Frankhauser, P. & Biernacki, C. (2008). The morphology of built-up landscapes in Wallonia, Belgium: a classification using fractal indices. *Landscape and Urban Planning*, 84, 99–115
- Thomas, I., Frankhauser, P., Frenay, B. & Verleysen, M. (2010). Clustering patterns of urban built-up areas with curves of fractal scaling behaviour, *Environment and Planning B: Planning and Design*, 37, 942–954.
- Vicsek, T. (1990). Mass multifractals. *Physica A: Statistical Mechanics and its Applications*, 168(1), 490–497.